Secure Energy-Efficient Multi-RIS-aided SWIPT Networks

Chukwuemeka Nwufo, Yichuang Sun, and Oluyomi Simpson

School of Physics, Engineering and Computer Science
University of Hertfordshire, Hatfield, Hertfordshire, AL10 9AB, United Kingdom.
cn18abe@herts.ac.uk, y.sun@herts.ac.uk, and o.simpson@herts.ac.uk

***Abstract*— This paper considers a SWIPT network in which an access point (AP) serves multiple information decoding receivers (IDRs) and energy harvesting receivers (EHRs) assisted by several dynamically controlled reconfigurable intelligent surfaces (RIS). An energy efficiency (EE) maximization problem is formulated by the joint optimization of the transmit beamforming, artificial noise (AN) covariance, the passive beamforming at the RISs, and the RIS on/off control mechanism. Due to the non-convexity of the problem, semi-definite relaxation (SDR) is utilized to simplify the problem. A practical solution based on alternation optimization is proposed to obtain the suboptimal solution. Furthermore, a low-complexity greedy search method is proposed for the RIS on/off control. Simulation results show that the EE is significantly enhanced by employing dynamic control of multiple RIS with AN. In addition, the effect of increasing the circuit power and the number of RISs can be harmful to the system-wide EE.**

Index terms—Reconfigurable intelligent surfaces, energy efficiency, artificial noise, SWIPT

I. INTRODUCTION

The concept of Simultaneous wireless information and power transfer (SWIPT) has been met with explosive interest due to their potential to extend the network lifetime and improve energy efficiency, especially in low-power Internet of Things (IoTs) devices in 5G networks and beyond [1]. SWIPT allows wireless nodes to utilize the RF signal for simultaneous wireless information and power transfer. Furthermore, SWIPT enables wireless nodes to utilize the RF signal for both wireless information transfer (WIT) and wireless power transfer (WPT) simultaneously [2][3]. Conventional SWIPT architectures allow for two different design types: the co-located and separated receiver modules for information decoding (ID) and energy harvesting (EH).

Recently, several 5G technological advancements such as Millimetre-wave (mm-Wave) communications and massive-multiple input-multiple output (mMIMO) technology have been projected to meet a thousand-fold capacity increase and provide ubiquitous wireless connectivity to a variety of devices [4]. However, these advancements exhibit several shortcomings in energy efficiency and hardware cost, and practical implementations may prove very prohibitive. Therefore, a more energy-efficient and cost-effective technology that has emerged to plug the gaps presented by the technologies mentioned above while still offering significant gains is the reconfigurable intelligent surface (RIS), also called the intelligent, reflective surfaces (IRS). A RIS is an artificial structure that can be electronically tuned using integrated electronics and wireless communications [6]. The 2-dimensional surface has many low-cost, reconfigurable passive elements that can independently induce a phase shift on impinging waves. Furthermore, proper tuning of the surface impedances of the surface elements enables the phase shifts to be adjusted to allow for the coherent addition of the reflected signal from these elements to boost the desired signal at the designated receiver [7]– [10].

The main bane of wireless communication is the open access nature. Therefore, the wireless communication system requires strong security measures at all layers of its protocol stack to combat the risks associated with the open-access attribute. Cryptographic encryptions are often used in higher layers of the protocol stack [10], [11], while security at the informatic theoretic physical layer has become equally important. Physical layer security (PLS) exploits the eavesdropper channel state information (CSI) and that of the legitimate parties to provide some form of security and confidentiality [12], [14], [15]. A typical SWIPT system with separated receivers has EHRs with different power sensitivity from the IDRs. As such, the EHRs are deployed closer to the AP while the IDRs are further away. This implies a stronger line-of-sight (LoS) between EHR and AP compared to the IDR. As a result, there could be a degradation in the overall spectral efficiency of the system. Furthermore, there could be a breach of confidentiality of the information received by the IDRs. Therefore, employing a RIS to aid the SWIPT network can significantly enhance the network-wide performance. Several studies have shown the performance enhancements of RIS-aided SWIPT systems over conventional RIS systems. For example, the authors in [16] studied a power minimization problem under the quality of service (QoS) constraints. They showed that the RIS-aided SWIPT system performed better than the conventional SWIPT system. Furthermore, in [4], the authors studied a weighted sum maximization problem for a RIS-aided SWIPT system by jointly optimizing the transmit precoders at the AP and the random phase shifts at the RIS.

This work aims to improve the energy efficiency, η, of a multi-RIS-aided SWIPT network where a multiple antenna access point (AP) serves several IDRs and EHRs via one direct channel and multiple RIS channels. It does this while preventing the EHRs from eavesdropping on the transmitted information from the IDRs. To achieve this, we employ a non-linear energy-harvesting model [17] rather than a linear one [16] to characterize the harvested energy more accurately. Furthermore, we aim to maximize the system-wide energy efficiency, η, by jointly optimizing the transmit beamforming vectors, the artificial noise (AN) covariance matrix at the AP and the phase shifts at the RIS.

II. SYSTEM MODEL

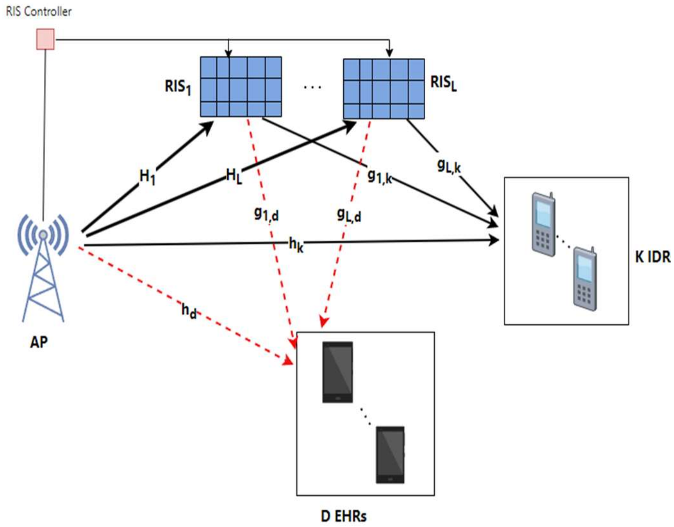

Fig.1: Diagrammatic representation of the multi-RIS-aided SWIPT

Fig. 1 depicts a multi-RIS-aided SWIPT system in which an access point with M antenna serves a SWIPT system with a set of K IDRs and D EHRs, each equipped with a single antenna. The service is via direct links and a set of L RIS links. Each RIS is composed of N number of reflecting elements. The mixed transmitted signal is given as

$$x = \sum_{k=1}^{K} \boldsymbol{v_k} s_k + \boldsymbol{v_0} \tag{1}$$

where $\boldsymbol{v_k} \in \mathbb{C}^{M\times 1}$ and $s_k \sim \mathcal{C}(0,1)$ with $\mathbb{E}\{|s_k|^2\} = 1$ are the beamforming vector and the confidential information signal for *k-th* IDR. $\boldsymbol{v_0} \in \mathbb{C}^{M\times 1}$ denotes the artificial noise with $\boldsymbol{v_0} \sim \mathcal{C}(0, \boldsymbol{V_0})$.

The received signal at the IDR, *k,* is given by

$$y_k = \underbrace{\left(\boldsymbol{h_k^H} + \sum_{l=1}^{L} b_l \boldsymbol{g_{l,k}^H \Phi_l H_l}\right)}_{\bar{\boldsymbol{h}}_k^H} x + n_k \tag{2}$$

where $\boldsymbol{h_k^H} \in \mathbb{C}^{\boldsymbol{M\times 1}}$ is the channel vector between the AP and IDR, k, $\boldsymbol{g_{l,k}^H} \in \mathbb{C}^{\boldsymbol{N\times 1}}$ is the channel vector from the *l-th* RIS to IDR, k; therefore $\boldsymbol{g_k^H} = [\boldsymbol{g_{1,k}^H}, \boldsymbol{g_{2,k}^H}, \dots \boldsymbol{g_{L,k}^H}]$. Similarly, $\boldsymbol{H_l} \in \mathbb{C}^{\boldsymbol{N\times M}}$ is the channel matrix from the AP to the *l-th* RIS. $\boldsymbol{\Phi_l} \in \mathbb{C}^{\boldsymbol{N\times N}}$ is the phase shift matrix of the *lth* RIS given by $\boldsymbol{\Phi_l} = diag(\phi_l)$ where $\boldsymbol{\phi_l} = [e^{j\theta_1}, e^{j\theta_2}, \dots, e^{j\theta_N}]^H{}_l$ and $\boldsymbol{\phi} = [e^{j\theta_{1,1}}, \dots, e^{j\theta_{1,N}}, \dots, e^{j\theta_{L,N}}]^H$ where $\theta_{l,n} \in [0, 2\pi]$ is the phase shift of the *n-th* element of the *l-th* RIS. $n_k \sim \mathcal{CN}(0, \sigma^2)$ is the additive white Gaussian noise (AWGN) at the *k-th* IDR.

Similarly, the received signal at the *d-th* EHR is given by

$$y_d = \underbrace{\left(\boldsymbol{h_d^H} + \sum_{l=1}^{L} b_l \boldsymbol{g_{l,d}^H \Phi_l H_l}\right)}_{\bar{\boldsymbol{h}}_d^H} x + \boldsymbol{n_d} \tag{3}$$

where $\boldsymbol{h_d^H} \in \mathbb{C}^{\boldsymbol{M\times 1}}$ is the channel matrix between the AP and the *d-th* EHR, $\boldsymbol{g_{l,d}^H} \in \mathbb{C}^{\boldsymbol{N\times 1}}$ is the channel matrix from the *lth* RIS to *d-th* EHR, $n_d \sim \mathcal{CN}(0, \sigma^2)$ is the AWGN noise at the *d-th* EHR.

Consequently, the received signal-to-interference-plus-noise-ratio (SINR) at the *k-th* IDR is given by:

$$\Gamma_k = \frac{\left\|\bar{\boldsymbol{h}}_{\boldsymbol{k}}^{\boldsymbol{H}} \boldsymbol{v_k}\right\|^2}{\bar{\boldsymbol{h}}_{\boldsymbol{k}}^{\boldsymbol{H}} \boldsymbol{V_0} \bar{\boldsymbol{h}}_{\boldsymbol{k}} + \sum_{j=1, j\neq k}^{K} \left|\bar{\boldsymbol{h}}_{\boldsymbol{j}}^{\boldsymbol{H}} \boldsymbol{v_j}\right|^2 + \sigma^2} \tag{4}$$

Thus, the achievable rate of the *k-th* IDR

$$r_k = \log_2(1 + \Gamma_k) \tag{5}$$

The achievable sum rate of all the K IDRs is given by

$$R \triangleq \sum_{k\in K} \log_2(1 + \Gamma_k) \tag{6}$$

Additionally, if the *d-th* EHR tries to decode information from its received signals, the receive SINR for eavesdropping on the information of IDR k is given by:

$$\Gamma_d = \frac{\left\|\bar{\boldsymbol{h}}_{\boldsymbol{d}}^{\boldsymbol{H}} \boldsymbol{v_k}\right\|^2}{\bar{\boldsymbol{h}}_{\boldsymbol{d}}^{\boldsymbol{H}} \boldsymbol{V_0} \boldsymbol{h_d} + \sum_{j=1, j\neq k}^{K} \left|\bar{\boldsymbol{h}}_{\boldsymbol{d}}^{\boldsymbol{H}} \boldsymbol{v_j}\right|^2 + \sigma^2} \tag{7}$$

Also, the harvested power at the *d-th* EHR is given by:

$$\Lambda_d = \eta_0 \left(\boldsymbol{h_d^H} \left(\sum_{k=1}^{K} \boldsymbol{v_k v_k^H} + \mathrm{Tr}(\boldsymbol{V_0}) \right) \boldsymbol{h_d} \right) \tag{8}$$

where η_0 is the energy harvesting efficiency ($\eta_0 = 1$) in this paper. To precisely characterize the harvested energy, we adopt a linear model as in [4],[16],[9].

$$\Psi = \sum_{d=1}^{D} \Lambda_d \tag{9}$$

Therefore, the total system-wide power requirement is given by

$$P_T = \vartheta \underbrace{\left(\sum_{k=1}^{K} \|v_k\|^2 + Tr(\boldsymbol{V_0}) \right)}_{} + \left(P_{AP} + \sum_{\boldsymbol{k=1}}^{\boldsymbol{K}} P_k \right) + \sum_{l=1}^{L} (b_l N P_r) - \Psi \tag{10}$$

The first term of (10) is the transmit power at the AP, where ϑ denotes the power amplifier efficiency. The second bracketed term is the circuit power consumption at the AP and the K IDRs, where P_k denotes the circuit power consumption at the *k-th* IDR, while the last term represents the power consumption of all RISs with P_r, the power requirement of a single element of the *l-th* RIS.

Consequently, we can define energy efficiency, $\boldsymbol{\eta}$ as

$$\boldsymbol{\eta} = \frac{R(\{\boldsymbol{v_k}\}, \boldsymbol{V_0}, \boldsymbol{\theta}, \boldsymbol{b})}{P_T(\{\boldsymbol{v_k}\}, \boldsymbol{V_0}, \boldsymbol{b})} \tag{11}$$

III. PROBLEM FORMULATION

Our multi-RIS SWIPT system design aims to maximize the overall energy efficiency subject to several constraints. Such constraints include the transmit power budget, minimum rate and security requirements of the IDRs, energy harvesting requirements of the EHRs, phase shifting restrictions on all the RIS and the ON/OFF basis for the RIS. Mathematically, we can express the optimization problem as:

$$\boldsymbol{P1}: \quad \max_{\{\{\boldsymbol{v_k}\}, \boldsymbol{V_0}\}, \boldsymbol{\theta}, b} \boldsymbol{\eta} \tag{12a}$$

$$\sum_{k=1}^{K} \|\boldsymbol{v_k}\|^2 + \mathrm{Tr}(\boldsymbol{V_0}) \le P_{max} \quad (12b)$$

$$\Gamma_k \ge \Gamma_{min} \quad \forall\, k \in K \quad (12c)$$

$$\Gamma_d \le \tau_{Th} \quad \forall\, d \in D, k \in K \quad (12d)$$

$$P_d \ge E_0 \quad \forall d \in D \quad (12e)$$

$$0 \le \theta_{l,n} \le 2\pi \quad \forall\, l \in L, n \in N \quad (12f)$$

$$b_l \in \{0,1\} \ \forall l \in L \quad (12g)$$

where $\boldsymbol{\theta} = [\theta_{1,1}, \dots, \theta_{1,N} \dots, \theta_{L,N}]^T$ and $\boldsymbol{b} = [b_1, \dots, b_L]^T$

The P_{max} in (12b) denotes the maximum available power at the AP, Γ_{min} in (12c) is the minimum SINR requirement of each IDR, and τ_{Th} in (12d) is the SINR threshold requirement for the EHR to successfully decode the confidential information meant for the IDRs. If both (12c) and (12d) are satisfied, the minimal requirement for the confidentiality of the IDR's information is guaranteed. In constraint (12e), E_0 denotes the minimal energy harvesting requirement at each EHR. The constraint (12g) is simply a binary representation of the ON/OFF mechanism for the RISs. **P1** is intractable since the objective problem is fractional and constraints (12e) to (12g) are non-convex.

IV. PROPOSED SOLUTION

Given the multiuser nature of the system, there is bound to be inter-user interference. Considering the multivariate optimization problem, we propose a low-complexity algorithm based on alternating optimization for the beamforming vectors, the phase shifts and the RIS on/off vector. The solution to (**P1**) will take a 3-pronged approach in which we will start by keeping both the RISs' phase shifts and on/off vectors fixed and then solve for the beamforming vectors. Secondly, keeping the RIS on/off vector fixed with the obtained beamforming vectors, we will solve for the optimization for the phase shifts. Finally, we will utilize the optimized beamforming vectors and the phase shifters to solve for the RIS ON/OFF vector. However, before applying this 3-pronged approach, we will use semi-definite relaxation to handle the non-convexity of (12).

i. Proposed SDR approach

To effectively solve **P1**, we need to transform the expression $\sum_{l=1}^{L} b_l \boldsymbol{g}_{l,k}^H \boldsymbol{\Phi}_l \boldsymbol{H}_l$. We can define $(\phi_n)_l = \left(e^{j\theta_n}\right)_l$; $\boldsymbol{\phi_l} = [\boldsymbol{\phi_{l1}}, \boldsymbol{\phi_{l2}}, \dots, \boldsymbol{\phi_{lN}}]^T$ and $\boldsymbol{\phi} = [\phi_{11}, \dots, \phi_{1N}, \dots, \phi_{LN}]^T$ with $\boldsymbol{b} = [b_1, \dots, b_L]^T . \forall l \in \mathcal{L}, n \in N$. Also, we recall that $\boldsymbol{H} = [\boldsymbol{H_1}, \dots, \boldsymbol{H_L}]^T \in \mathbb{C}^{N \times L \times M}$ and $\boldsymbol{\bar{H}} = \boldsymbol{b^T}.\boldsymbol{H}$ to cater for the RIS status. Furthermore, we define the vector $\boldsymbol{g_k} = [g_{1,1}, \dots, g_{l,n}, \dots, g_{L,N}]_{\boldsymbol{k} \in \boldsymbol{K}} \in \mathbb{C}^{(\boldsymbol{NL}) \times \boldsymbol{1}}$. Let $\boldsymbol{G_k} = diag[\boldsymbol{g_k}^{\boldsymbol{H}}]\boldsymbol{\bar{H}}$.

We will define new variables: $\boldsymbol{\bar{\phi}} = [\boldsymbol{\phi}; 1]$, $\boldsymbol{\bar{G}_k} = [\boldsymbol{G_k};\, \boldsymbol{h_k^H}]$and $\boldsymbol{\bar{G}_d} = [\boldsymbol{G_d};\, \boldsymbol{h_{d,k}^H}]$.We also set $\boldsymbol{v_k v_k^H} = \boldsymbol{V_k}$ satisfying $\boldsymbol{V_k} \succcurlyeq 0$ and $rank(\boldsymbol{V_k}) = 1$. In the same vein, we set $\boldsymbol{Q} = \boldsymbol{\bar{\phi}}\boldsymbol{\bar{\phi}}^H$ satisfying $\boldsymbol{Q} \succcurlyeq 0$ and $rank(\boldsymbol{Q}) = 1$. To represent all the phase shifts for all the RIS, we assume that $\overline{W} = L \times N$, and to cater for the ON/OFF status of the RIS, we assume $W = b^T.\overline{W}$. Also, we let $\boldsymbol{\bar{V}_j} = \boldsymbol{V_0} + \sum_{\substack{j=1 \\ j \ne k}}^{K} \boldsymbol{V_j}$. Thus, we can rewrite the sum rate as

$$R_T = \sum_{k=1}^{K} \log_2\left(1 + \frac{\mathrm{Tr}\left(\boldsymbol{Q\bar{G}_k V_k \bar{G}_k}^{\boldsymbol{H}}\right)}{\mathrm{Tr}\left(\boldsymbol{Q\bar{G}_k}(\boldsymbol{\bar{V}_j})\boldsymbol{\bar{G}_k}^{\boldsymbol{H}}\right) + \sigma^2}\right) \quad (13)$$

Therefore, we can relax the optimization problem (**P1**) to the formulation below with SDR by dropping the rank one constraint.

$$\boldsymbol{P2}: \max_{\{\{\boldsymbol{V_k}\},\boldsymbol{V_0}\},\boldsymbol{Q}} \boldsymbol{\eta} \quad (14a)$$

$$\text{s.t} \quad \boldsymbol{V_k}, \boldsymbol{V_0},\ \boldsymbol{Q_{ww}} \succcurlyeq 0 \forall\, k, w = 1, \dots, W+1 \quad (14b)$$

$$\sum_{k=1}^{K} \mathrm{Tr}(\boldsymbol{V_k}) + \mathrm{Tr}(\boldsymbol{V_0}) \le P_{max} \quad (14c)$$

$$\frac{\mathrm{Tr}\left(\boldsymbol{Q\bar{G}_k V_k \bar{G}_k}^{\boldsymbol{H}}\right)}{\mathrm{Tr}\left(\boldsymbol{Q\bar{G}_k}(\boldsymbol{\bar{V}_j})\boldsymbol{\bar{G}_k}^{\boldsymbol{H}}\right) + \sigma^2} \ge \Gamma_k \quad (14d)$$

$$\frac{\mathrm{Tr}\left(\boldsymbol{Q\bar{G}_d V_k \bar{G}_d}^{\boldsymbol{H}}\right)}{\mathrm{Tr}\left(\boldsymbol{Q\bar{G}_d}(\boldsymbol{\bar{V}_j})\boldsymbol{\bar{G}_d}^{\boldsymbol{H}}\right) + \sigma^2} \le \tau_{Th} \quad (14e)$$

$$\mathrm{Tr}\left(\boldsymbol{Q\bar{G}_d}\left(\sum_{k=1}^{K} \boldsymbol{V_k} + \boldsymbol{V_0}\right)\boldsymbol{\bar{G}_d}^{\boldsymbol{H}}\right) \ge \boldsymbol{Z}^{-1}(p_d) \quad (14f)$$

ii. Beamforming optimization

We will start by keeping $\boldsymbol{Q}$ fixed and optimizing $\{\{\boldsymbol{V_k}\}, \boldsymbol{V_0}\}$. Thus, the optimization problem, **P2**, is transformed to

$$\boldsymbol{P3}: \max_{\{\boldsymbol{V_k},\boldsymbol{V_0},\boldsymbol{S}\}} \frac{\sum_{k=1}^{K} \log_2(1 + S_k)}{P_T(\{\boldsymbol{V_k}\}, \boldsymbol{V_0})} \quad (15a)$$

$$s.t. \quad (14b) – (14e)$$

$$\boldsymbol{V_k}, \boldsymbol{V_0} \succcurlyeq 0, \quad \forall k \quad (15b)$$

$$\Gamma_k \ge S_k \quad \forall k \quad (15c)$$

where $\boldsymbol{S} = [S_1, \dots, S_k, \dots, S_K]^T$ are slack variables to ensure that the constraint (15c) holds with equality to obtain the optimal solution.

To effectively handle the non-convex constraint in (15c), we can break it down into the following set of expressions:

$$\mathrm{Tr}(\boldsymbol{A_k V_k}) \ge S_k\left(\mathrm{Tr}\left(\boldsymbol{A_k}(\boldsymbol{\bar{V}_j})\right) + \sigma^2\right) \quad (16a)$$

$$\mu_k \ge \mathrm{Tr}\left(\boldsymbol{A_k}(\boldsymbol{\bar{V}_j})\right) \quad \forall k \quad (16b)$$

where $\mu_k$is an auxiliary variable and $\boldsymbol{A_k} = \boldsymbol{\bar{G}_k Q \bar{G}_k}^{\boldsymbol{H}}$. Thus, we can redefine the set of constraints in (16) as follows:

$$S_k \le e^{\alpha_k} \text{ and } \mu_k \le e^{\beta_k}\ \forall k \in K \quad (17a)$$

$$\mathrm{Tr}(\boldsymbol{A_k V_k}) \ge e^{\alpha_k}\left(e^{\beta_k} + \sigma^2\right) = e^{\alpha_k + \beta_k} + \sigma^2 e^{\alpha_k} \quad (17b)$$

where $\alpha_k$and β_k are auxiliary variables.

Without loss of generality, we can equate the lower bound of the left-hand side of the two expressions in (17a) to the first-order Taylor series expansion at any feasible point $[\alpha_0, \beta_0]$ such that $e^{\alpha_k} \ge e^{\alpha_0} + e^{\alpha_0}(\alpha_k - \alpha_0)$ and $e^{\beta_k} \ge e^{\beta_0} + e^{\beta_0}(\beta_k - \beta_0)$. Thus, given the above approximation in (17a & b) as well as Taylor's series expansions, we can obtain a lower bound solution to **P3** by solving the following:

$$\boldsymbol{P4}: \max_{\{\boldsymbol{V_k},S_k,\alpha_k,\beta_k\}} \frac{\sum_{k=1}^{K}(1+S_k)}{P_T(\{\boldsymbol{V_k}\},\boldsymbol{V_0})} \quad (18a)$$

$$s.t \quad (15b), (15c), (17b), \boldsymbol{V_k}, \boldsymbol{V_0} \succcurlyeq 0,\ \forall k \quad (18b)$$

$$f_0(\alpha_k) \ge \mathrm{Tr}\left(\boldsymbol{A_k \bar{V}_j}\right)\ \forall k \quad (18c)$$

$$f_0(\beta_k) \ge S_k\ \forall k \quad (18d)$$

where $f_0(\alpha_k) \triangleq e^{\alpha_0} + e^{\alpha_0}(\alpha_k - \alpha_0)$ and $f_0(\beta_k) \triangleq e^{\beta_0} + e^{\beta_0}(\beta_k - \beta_0)$.

Given that the numerator of the objective function in **P4** is concave while the denominator is convex, we can employ the Dinkelbach method [15] to solve the problem in polynomial time. The Dinkelbach method guarantees that we obtain the globally optimal solution of **P4** if and only if λ is the unique zeroth solution to the function in the following problem:

$$\max_{\{\{,\{\boldsymbol{V_k}\},\boldsymbol{S},\boldsymbol{\mu}\},\boldsymbol{V_0}\}} F_o(\lambda) \tag{19a}$$

$$\text{s.t.} \quad \text{(14a-e), (18c), (18d)}, \ \boldsymbol{V_k}, \boldsymbol{V_0} \succcurlyeq 0, \ \forall k \tag{19b}$$

where $F_o(\lambda) = \sum_{k=1}^{K}(1 + S_k) - \lambda\left(P_T(\{\boldsymbol{V_k}\}, \boldsymbol{V_0})\right)$

Algorithm 1 below describes the Dinkelbach method to solve **P4**, which we can solve using convex solvers such as CVX [19]. By algorithm I, we can solve the optimization problem **P3** using successive convex approximation (SCA) by iteratively solving **P4** with $[\alpha_0, \beta_0]$ until the difference between successive iterations is below a tolerance value, ε.

ALGORITHM I: SOLUTION TO P4

1. **Initialize**: Set initial values for $\alpha_k$and β_k to ${\alpha_0}^{(0)}$and ${\beta_0}^{(0)}$ respectively. Set $\lambda^{(0)} = 0, \varepsilon$=small tolerance value and iteration count, $i = 0$.
2. Repeat
3. Solve (19) with $\lambda^{(i)}$and $\{{\alpha_0}^{(i)}, {\beta_0}^{(i)}\}$ to obtain ${\boldsymbol{V_k}}^{(i)}, {\boldsymbol{V_0}}^{(i)}$ and $F_o(\lambda^{(i)})$.
4. Set $\lambda^{(i+1)} = \frac{\sum_{k=1}^{K}(1+S_k)}{\vartheta \sum_{k=1}^{K}\text{Tr}(\boldsymbol{V_k}) + \text{Tr}(\boldsymbol{V_0}) + P_c + \sum_{l=1}^{L} b_l N_l P_r}$
5. $i \leftarrow i + 1$
6. Until $H_o(\lambda^{(i)}) \le \varepsilon$
7. **Output**: The optimal ${\boldsymbol{V_k}}^* = {\boldsymbol{V_k}}^{(i)}$and ${\boldsymbol{V_0}}^{(*)} = {\boldsymbol{V_0}}^{(i)}$

iii. Phase Optimization with fixed $\{\{\boldsymbol{V_k}\}, \boldsymbol{V_0}\}$

To optime the phase shift, we will keep the obtained $\{\{\boldsymbol{V_k}\}, \boldsymbol{V_0}\}$ fixed. Thus, the optimization problem (**P2**) reduces to

$$\boldsymbol{P5}: \quad \max_{\boldsymbol{Q}\succcurlyeq\boldsymbol{0},\{\rho_k\}} \frac{\sum_{k=1}^{K}\log_2(1 + \rho_k)}{P_T(\{\boldsymbol{V_k}\}, \boldsymbol{V_0})} \tag{20a}$$

$$s.t. \ \text{(14b) – (14e)}, \tag{20b}$$

$$\boldsymbol{Q_{ww}} = 1 \quad \forall\, w = 1, \dots, W + 1 \tag{20c}$$

$$\Gamma_k \ge \rho_k \qquad \forall k \tag{20d}$$

where ρ_k are auxiliary variables.

Consequently, we can transform the **P5** to

$$\boldsymbol{P6}: \quad \max_{\boldsymbol{Q}\succcurlyeq\boldsymbol{0},\{\rho_k,\mu_k,\omega_k\}} \frac{\sum_{k=1}^{K}\log_2(1 + \rho_k)}{P_T(\{\boldsymbol{V_k}\}, \boldsymbol{V_0})} \tag{21a}$$

$$s.t. \ \text{(14b) – (14e)} \tag{21b}$$

$$\boldsymbol{Q_{ww}} = 1 \quad \forall\, w = 1, \dots, W + 1 \tag{21c}$$

$$\text{Tr}(\boldsymbol{X_k Q}) \ge e^{\mu_k + \omega_k} + \sigma^2 e^{\omega_k} \tag{21d}$$

$$f_0(\mu_k) \triangleq e^{\mu_0} + e^{\mu_0}(\mu_k - \mu_0) \ge \text{Tr}(\boldsymbol{Y_k Q}) \quad \forall k \tag{21e}$$

$$f_0(\omega_k) \triangleq e^{\omega_0} + e^{\omega_0}(\omega_k - \omega_0) \ge \rho_k \ \forall k \tag{21f}$$

where $\boldsymbol{X_k} = \boldsymbol{\overline{G}_k}\, \boldsymbol{V_k}{\boldsymbol{\overline{G}_k}}^{\boldsymbol{H}}$ and $\boldsymbol{Y_k} = \boldsymbol{\overline{G}_k}\, (\boldsymbol{\overline{V}_j}){\boldsymbol{\overline{G}_k}}^{\boldsymbol{H}}$.

μ_k and ω_k are auxiliary variables with $\{\mu_0, \omega_0\}$ denoting any set of feasible points. $f_0(\mu_k)$ and $f_0(\omega_k)$ are the lower-bounded expressions of the first-order Taylor's expansion of the functions, e^{μ_k} and e^{ω_k} at feasible point (μ_0, ω_0).

P6 is convex and can be solved using any convex solvers. Similarly, we can quickly solve the optimization problem **P5** by employing SCA and iteratively solving **P6** with the feasible point at $\{\mu_0, \omega_0\}$ until the difference between successive approximations is below a certain threshold.

iv. RIS on/off vector optimization

Having obtained the beamforming and phase shift vectors ($\{\{\boldsymbol{V_k}\}, \boldsymbol{V_0}\}$, and $\boldsymbol{\phi}$), and applying them to the optimization problem (11), the equation reduces to a non-linear optimization problem (NLOP) with respect to the RIS on/off vector, ***b***. Unfortunately, this makes obtaining a globally optimal solution in polynomial time increasingly tricky, given that the problem is generally NP-hard. To effectively solve the NLOP, we draw inspiration from [16] to propose a low-complex greedy algorithm such that we aim to obtain a feasible solution to the system-wide energy efficiency optimization problem **P2** by turning off one RIS at a time. Each time a feasible solution is obtained, it is compared to the previous solution until we find a solution that ultimately improves the energy efficiency. Algorithm II defines this scenario in full detail.

ALGORITHM II: GREEDY ALGORITHM FOR RIS ON/OFF OPTIMIZATION

1. Let L be the set of all RISs and initialize RIS status $\boldsymbol{b} = \{b_1, \dots, b_L\}$ with $b_l = 1 \ \forall l \in L$
2. Initialize a subset C (initially empty) for only RISs, $\rightarrow C \in L$
3. Solve **P1** and find the solution to the objective function in the optimization problem (12), and denote the solution by $\boldsymbol{\eta_0}$
4. **while** C is not empty:
   for each l in C:
   Construct a RIS ON/OFF solution sequence as follows: set $b_l = 0, b_l = 1, b_l = 0 \ \forall l, m, n \in L$
5. **Feasibility check:**
   - If the RIS ON/OFF solution sequence is feasible, compute the objective function in (12) as $\boldsymbol{\eta_l}$
   - Otherwise, set $\boldsymbol{\eta_l} = 0$
6. **end** for
7. Compare $\boldsymbol{\eta_l}$ and $\boldsymbol{\eta_0}$ and find $x = arg \max_{j \in C} \boldsymbol{\eta_j}$
8. If $x \neq 0$, then
   Set $C = C \backslash \{x\}$ and $\boldsymbol{\eta_0} = \boldsymbol{\eta_x}$
9. **Else**
10. Break and jump to step (13)
11. end if
12. end while
13. Output: $b_l = 1, b_m = 0 \ \forall l \in \ C \ and \ \forall m \in L \backslash C$

Hence, the AO algorithm is summarized in Algorithm III.

v. Computational complexity

The number of iterations of the AO process in algorithm VI determines the computational complexity of the multiuser system. We can denote this number by $N_{iter}^{(AO)}$. The computational complexity of the solution at hand is drawn from the complexity of solving three (3) sub-problems, which we will discuss in batches. The first batch considers the complexity of (15) when the RIS on/off vector is fixed. From algorithm I, we can observe an outer loop SCA and an inner loop, which adopts the Dinkelbach method for solving **P3**. We adopt the interior point method (IPM) to solve (19) at each iteration. We can define the number of iterations of the outer loop as $N_{iter}^{(SCA_1)}$ and the inner loop as $N_{iter}^{(D_1)}$. Also, as defined in [17], the complexity of solving a constrained optimization problem is dependent on the number of optimization variables and the constraints. Thus, the complexity of solving (19) is in the order $O_1 = O\left(\sqrt{(K+1)M+\mathcal{Y}}\left(\mathcal{X}_1^{\,2}\left(\mathcal{Y}+(K+1)M^2+\mathcal{X}_1(\mathcal{Y}+(K+1)M^3+\mathcal{X}_1^{\,3})\right)\right)\right)$ where $\mathcal{X}_1 = O(KM^2)$ and $\mathcal{Y} = (KW+4K+D+1)$. Similarly, we can define the number of iterations for solving SCA in **P5** as $N_{iter}^{(SCA_2)}$. At each iteration, the complexity of solving the convex problem **P6** is given by $O_2 = O\left(\sqrt{(W+1)+\mathcal{Z}}\left(\mathcal{X}_2^{\,2}(\mathcal{Z}+(W+1)^2)+\mathcal{X}_2(\mathcal{Z}+(W+1)^3+\mathcal{X}_2^{\,3})\right)\right)$ where $\mathcal{X}_2 = O(W^3+3K)$ and $\mathcal{Z} = (5K+D+W+2)$. Also, the complexity of the RIS on/off optimization is given by $O_3 = O(W^2K)$ with $N_{iter}^{(g)}$ iterations. Thus, the overall complexity of the alternating optimization algorithm is given by $O_{OA} = O\left(N_{iter}^{(AO)}\left(N_{iter}^{(SCA_1)}.N_{iter}^{(D_1)}.O_1+N_{iter}^{(SCA_2)}O_2+N_{iter}^{(g)}\,O_3\right)\right)$

Thus, the implication is that the proposed algorithm has polynomial time computational complexity.

ALGORITHM III: OVERALL SOLUTION FOR P1

1. Initialize $(\{\{\boldsymbol{V}_k\},\boldsymbol{V}_0\}^{[0]},\ \boldsymbol{\phi}^{[0]},\boldsymbol{b}^{[0]})$. Set iteration number $i=0$
2. Repeat
3. Given $(\boldsymbol{\phi}^{[i-1]},b^{[i-1]})$, solve the optimization problem given in (15) using algorithm IV to obtain $\{\{\boldsymbol{V}_k\},\boldsymbol{V}_0\}^{[i]}$
4. Given $\left(\{\{\boldsymbol{V}_k\},\boldsymbol{V}_0\}^{[i]},b^{[i-1]}\right)$, solve the optimization problem given in (21) by using SCA to obtain $\boldsymbol{\phi}^{[i]}$
5. Given $(\{\{\boldsymbol{V}_k\},\boldsymbol{V}_0\}^{[i]},\ \boldsymbol{\phi}^{[i]})$, optimize the RIS on/off vector using algorithm V to obtain $\boldsymbol{b}^{[i]}$
6. Set $i=i+1$
7. Until the objective value of (13) converges

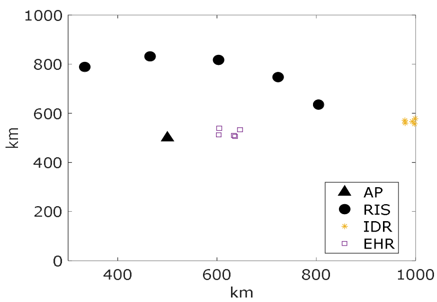

Fig 2: Multi-RIS-aided SWIPT setup

V. NUMERICAL RESULTS

This section evaluates the performance of the proposed multi-RIS (MRIS) algorithm. We consider $(1000\times1000)m^2$ square area with a 4-antenna AP located at its centre. The AP is circularly surrounded by L number RISs, each located at polar coordinates given by $\left[((\cos(2\pi lL^{-1}),\sin(2\pi lL^{-1}))\times 100)+[500,500]\right]$. The energy harvesting receivers are randomly placed within a 2500m^2 square space centred at (600,500) while the IDRs are further away, randomly distributed within a 2500m^2 square space centred at (950,550). The AP is assumed to transmit at maximum power. We also assume that the AP-EHR and AP-IDR links experience Rayleigh fading while AP-RISs, RISs-IDR and RISs-EHR channels experience Rician fading with a Rician factor, 4. All simulations were averaged over 500 independent channel realizations. Other system parameters are selected as follows: K=5, D = 5, $\sigma^2 = -174$dBm/Hz, power amplifier efficiency, $\vartheta = 0.8$, circuit power of each RIS element, $P_r = 10dBm$, $\tau_{Th} = 0dB$, $\Gamma_{min} = 5dB$, $E_0 = -25dBm$. We simulate three other schemes for performance comparisons: (a) ***Upper bound***: In this scheme, the energy efficiency is obtained from the relaxed problem in P2 by applying semi-definite relaxation; (b) ***Without AN***: This scheme eliminates the AN transmitted alongside the transmit signal; (c) ***Without RIS***: This scheme eliminates the cascaded AP-RIS and RIS -IDR links. Only the direct AP-IDR links are considered. Further comparisons are made to ascertain the performance enhancements of a multi-RIS system with a conventional single RIS and no RIS system.

Fig. 3 illustrates the average energy efficiency against the number of reflective elements per RIS for the different schemes, including our proposed MRIS design. Upon examination, we see that as the number of reflective elements increases per RIS, the energy efficiency increases and then gradually decreases with more reflective elements. The reason for such a behaviour is that in the initial phase, with a few reflective elements in each RIS, the active beamforming gain from the AP and reflecting beamforming gain of the RISs' phase shifts improve the spectral efficiency. This implies that the system-wide sum rate is enhanced. This significant sum rate overshadows the system-wide energy consumption, leading to increased energy efficiency. When the number of reflective elements in each RIS is relatively large, the information rate is enhanced but at the cost of increased energy consumption at the RISs. The plot shows that our proposed scheme posts similar energy efficiency performance as the upper bound and better performance than the other two schemes. The improved energy efficiency in our proposed system on the 'without AN' scheme is due to the EHRs compromising the information rate. Our scheme effectively applies the AN as energy beams for the EHRs. Moreover, the 'without AN' scheme outperforms the design without RIS; Hence, this provides an indication that an optimized RIS-assisted network enhances the performance of an AN-assisted network.

Fig. 4 depicts the energy efficiency versus the number of transmit antennas at the AP for different Pmax. The figure shows that energy efficiency increases rapidly for a small number of transmit antennas at the AP. Still, this increase becomes slower for a more significant number of transmit antennas at the AP. A high number of transmit antennas at the AP results in high power consumption, which depletes the slope of an increase in energy efficiency. Also, the energy efficiency increases with an increase in the maximum transmit power of the AP for a given number of transmit antennas at the AP. Fig. 5 presents a comparison of the energy efficiency obtained for the different schemes against the P_c (Recall that, from section II, P_c is the sum of the circuit power at the AP and the IDRs, which is incremental with the number of IDRs and antennas at the AP). We observe a negative slope in the figure because of the effect of total circuit power on energy efficiency. The energy efficiency decreases as a result of increasing circuit power. Our proposed scheme outperforms the single RIS (L=1) scheme and other schemes while it approaches the performance posted by the upper bound. This is consistent with the result obtained in Fig. 3. Lastly, Fig. 6 shows the average energy efficiency as a function of the number of RIS (N=4 for each RIS) for different maximum power levels at the AP. From the figure, we see that as L increases, there is a gradual increment in the average energy efficiency due to the RISs on the system-wide information rate. However, as the L becomes relatively large, the energy efficiency slowly decreases due to the energy consumption costs associated with the large number of RIS. Thus, we observe that the larger the maximum power at the AP is, the better the energy efficiency performance.

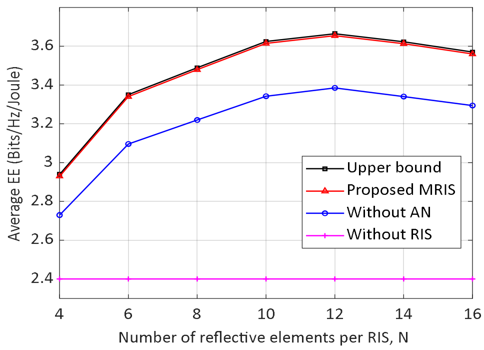

Fig 3: Average energy efficiency vs. the number of elements per RIS, N

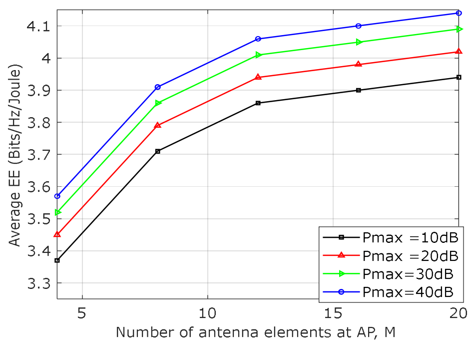

Fig 4: Average energy efficiency vs. the number of antenna elements at AP

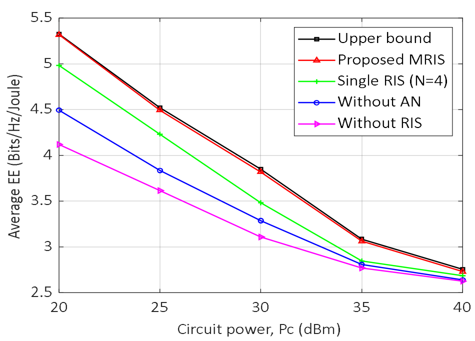

Fig 5: Average energy efficiency vs. the total circuit power, P_c

VI. CONCLUSION

This paper studied the energy efficiency of a secure distributed multi-RIS-aided SWIPT network. The non-convexity of the energy efficiency problem was overcome by applying SDR and tackling the resultant problem with AO to obtain an effective solution. Simulation results show the positive effect of RISs on the system's energy efficiency. Furthermore, multiple RIS deployed at different points can seemingly improve the energy efficiency of a SWIPT network over a single RIS or no RIS at all. Moreover, applying AN in the system improves its energy efficiency and security.

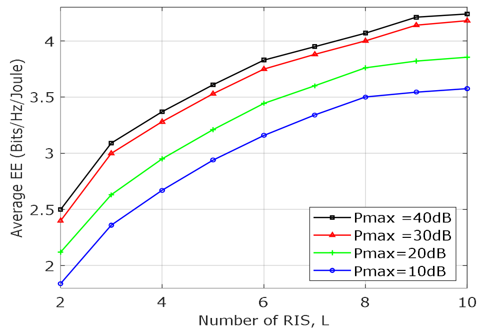

Fig 6: Average energy efficiency as a function of the number of RIS, L

REFERENCES

[1] J. Xu, L. Liu, and R. Zhang, "Multiuser MISO Beamforming for Simultaneous Wireless Information and Power Transfer," *IEEE Transactions on Signal Processing*, vol. 62, no. 18, Sep. 2014, doi: 10.1109/TSP.2014.2340817.

[2] NGMN Alliance, "6G Drivers and Vision by NGMN Alliance," Apr. 2021. Accessed: Mar. 14, 2022. [Online]. Available: www.ngmn.org

[3] A. Zappone, L. Sanguinetti, G. Bacci, E. Jorswieck, and M. Debbah, "Energy-Efficient Power Control: A Look at 5G Wireless Technologies," *IEEE Transactions on Signal Processing*, vol. 64, no. 7, pp. 1668–1683, Apr. 2016, doi: 10.1109/TSP.2015.2500200.

[4] F. Boccardi, R. W. Heath, A. Lozano, T. L. Marzetta, and P. Popovski, "Five disruptive technology directions for 5G," *IEEE Communications Magazine*, vol. 52, no. 2, Feb. 2014, doi: 10.1109/MCOM.2014.6736746.

[5] C. Huang, G. C. Alexandropoulos, A. Zappone, M. Debbah, and C. Yuen, "Energy Efficient Multiuser MISO Communication using Low-Resolution Large Intelligent Surfaces," Sep. 2018, [Online]. Available: http://arxiv.org/abs/1809.05397

[6] X. Li, C. Zhang, C. He, G. Chen, and J. A. Chambers, "Sum-Rate Maximization in IRS-Assisted Wireless Power Communication Networks," *IEEE Internet Things J*, vol. 8, no. 19, pp. 14959–14970, Oct. 2021, doi: 10.1109/JIOT.2021.3072987.

[7] A. Papazafeiropoulos, C. Pan, P. Kourtessis, S. Chatzinotas, and J. M. Senior, "Intelligent Reflecting Surface-assisted MU-MISO Systems with Imperfect Hardware: Channel Estimation, Beamforming Design," Feb. 2021, [Online]. Available: http://arxiv.org/abs/2102.05333

[8] J. Liu, K. Xiong, Y. Lu, D. W. K. Ng, Z. Zhong, and Z. Han, "Energy Efficiency in Secure IRS-Aided SWIPT," *IEEE Wireless Communications Letters*, vol. 9, no. 11, pp. 1884–1888, Nov. 2020, doi: 10.1109/LWC.2020.3006837.

[9] Y. Yang, S. Zhang, and R. Zhang, "IRS-Enhanced OFDM: Power Allocation and Passive Array Optimization," in *2019 IEEE Global Communications Conference (GLOBECOM)*, IEEE, Dec. 2019, pp. 1–6. doi: 10.1109/GLOBECOM38437.2019.9014204.

[10] K. Cumanan, R. Krishna, Z. Xiong, and S. Lambotharan, "SINR Balancing Technique and its Comparison to Semi-definite Programming Based QoS Provision for Cognitive Radios," in *VTC Spring 2009 - IEEE 69th Vehicular Technology Conference*, IEEE, Apr. 2009, pp. 1–5. doi: 10.1109/VETECS.2009.5073854.

[11] Yingbin Liang, H. V. Poor, and S. Shamai, "Secure Communication Over Fading Channels," *IEEE Trans Inf Theory*, vol. 54, no. 6, pp. 2470–2492, Jun. 2008, doi: 10.1109/TIT.2008.921678.

[12] C. E. Shannon, "Communication Theory of Secrecy Systems*," *Bell System Technical Journal*, vol. 28, no. 4, pp. 656–715, Oct. 1949, doi: 10.1002/j.1538-7305.1949.tb00928.x.

[13] Lun Dong, Zhu Han, A. P. Petropulu, and H. V. Poor, "Improving Wireless Physical Layer Security via Cooperating Relays," *IEEE Transactions on Signal Processing*, vol. 58, no. 3, Mar. 2010, doi: 10.1109/TSP.2009.2038412.

[14] Y. Sun, D. W. K. Ng, J. Zhu, and R. Schober, "Robust and Secure Resource Allocation for Full-Duplex MISO Multicarrier NOMA Systems," *IEEE Transactions on Communications*, vol. 66, no. 9, Sep. 2018, doi: 10.1109/TCOMM.2018.2830325.

[15] W. Dinkelbach, "On Non-linear Fractional Programming," *Manage Sci*, vol. 13, no. 7, Mar. 1967, doi: 10.1287/mnsc.13.7.492.

[16] Z. Yang *et al.*, "Energy-Efficient Wireless Communications with Distributed Reconfigurable Intelligent Surfaces," May 2020, [Online]. Available: http://arxiv.org/abs/2005.00269